

DIFFERENTIAL ELECTRIC FIELD SENSITIVE FIELD EFFECT TRANSISTOR

Characteristics, Modeling and Applications

Yehya H. Ghallab^{1,2} and Wael Badawy²

¹ Department of Biomedical Engineering, Helwan University, Cairo, Egypt

² Department of Electrical and Computer Engineering, University of Calgary, Calgary, Alberta, Canada

Keywords: Electric Field Sensor, CMOS technology, Electric Field, Field Effect Transistor, lab-on-a-chip, Integrated sensors.

Abstract: This paper presents the Differential Electric Field Sensitive Field Effect Transistor (DeFET) as a CMOS electric field sensor. The DeFET is based on a standard 0.18- μm Taiwan Semiconductor Manufacturing Company (TSMC) CMOS technology. This paper also presents the DeFET's DC and AC models. The experimental and simulation results which validate the different models of the DeFET are presented. Moreover, some applications of the DeFET on the biomedical and lab-on-a-chip are presented.

1 INTRODUCTION

The Differential Electric Field Sensitive Field Effect Transistor (DeFET) device is a new electric field sensor which can sense the electric field and convert the electric field into a corresponding electrical signal such as voltage or current (Ghallab et al., 2005) (Ghallab et al., 2006) Its physical structure has two adjacent gate terminals (Ghallab et al., 2005). With the split-gate structure, DeFET can sense the electric field which is perpendicular to the gate channels of the device. Using the DeFET, we can get direct real-time information about the electric field, and consequently, we can extract useful information such as identify and characterize the biological cells (Ghallab et al., 2006). Also, the DeFET can be simply integrated with the CMOS-based lab on a chip and read-out circuits. As a new device, the DeFET is not a standard device in the (Simulation Program with Integrated Circuit Emphasis) SPICE simulator libraries, so we need a macro model to evaluate the performance of circuits composed of DeFET and MOSFET devices.

In this paper, SPICE macro models (dc and ac models) of DeFET will be offered to evaluate the performance of the circuits. Also, some applications of the DeFET are presented.

This paper is constructed as follows. The operational principle of the DeFET is reviewed in part2. The SPICE macro models (dc and ac) are

formed and described in Section 3. Experimental and simulation results which confirm the proposed models are shown and discussed in part 4. Some applications of the DeFET are presented in part 5. Section 6 concludes this paper and discusses the merits of the proposed DeFET based on the experimental findings.

2 THE DeFET

The DeFET consists of two complementary eFETs, one of them is a P eFET type and the second is an N eFET type (Ghallab et al., 2006). The eFET structure is shown in Fig. 1. The eFET contains two split drains, two split gates and a single source, see Fig. 1.

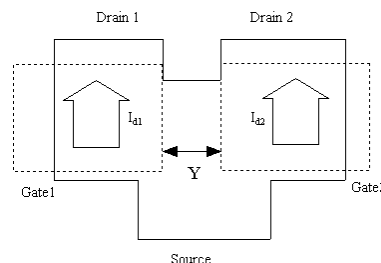


Figure 1: Schematic structure of an eFET.

The equivalent circuit of the DeFET is shown in Fig. 2.

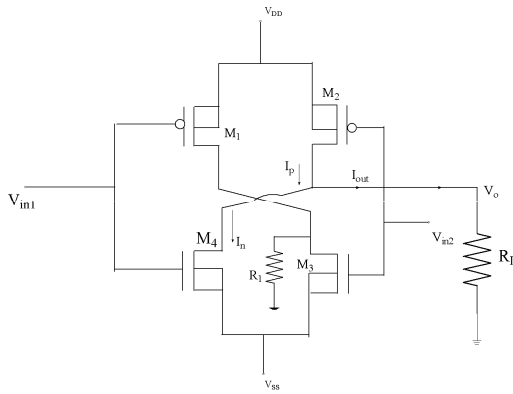


Figure 2: An equivalent circuit of a DeFET and schematic of the DeFET used in SPECTRE simulation.

From Fig. 2, the two gates of P eFET and N eFET are connected with each other, and there is a cross coupling between the two drains of the P eFET and the N eFET. The output current I_{Out} is equal to the difference between the two drain currents $I_p - I_n$ (i.e. $I_{Out} = I_p - I_n$, see Fig.2). On the other hand, I_p and I_n are functions of the two applied gate voltages V_{in1} and V_{in2} , respectively. The DeFET is designed to achieve an output voltage V_{Out} , directly related to the difference between the two applied gate voltages ($V_{in1} - V_{in2}$), and as $V_{in1} - V_{in2}$ is equal to the applied electric field above the two gates (E) multiplied by the distance between them ($V_{in1} - V_{in2} / Y = E$), where Y is the distance between the two split gates, which is constant. So, V_{Out} is related directly to the intensity of the applied electric field. Thus by measuring V_{Out} we can detect the intensity of the electric field to be as follows (Ghallab et al., 2006):

$$V_{Out} = g_m Y R_L E + V_{U_{ii}} \quad (1)$$

Eq. 1 shows a liner relationship between the DeFET's output voltage and the intensity of the applied electric field.

Also, from Eq. 1, we can observe that there is two cases, they are:

1) **Null electric-field case (Uniform case):** This special case will be obtained when the intensity of the electric filed is zero, and consequently getting the same potential on the two gates (i.e., $V_{in1} = V_{in2}$), and from Eq.1 $V_{out} = V_{uni}$

2) **Nonzero electric-field case (Nonuniform case):** This implies any electric-field condition that leads to a potential difference between the two gates (i.e., $V_{in1} \neq V_{in2}$). So, we can rewrite Eq. 1 as:

$$V_{out} = V_{Non} + V_{Uni} \quad (2)$$

where: $V_{non} = SE = g_m Y R_L E$ is the output voltage when we have a nonuniform electric field case, and V_{uni} is the output voltage when we have a uniform electric field case and S (sensitivity) = $g_m Y R_L$.

3 MODELING THE DeFET

As a new device, the DeFET is not a standard device in the simulator libraries, so a macro model to evaluate the performance of circuits composed of DeFET and MOSFET devices is needed. A Dc model has been proposed and tested using SPECTRE version 5. Also, an equivalent dc circuit of the DeFET using PSPICE version 9.1 have proposed. So, it can be used in the SPICE environment.

3.1 A Simple DC Model

Fig. 2 shows the proposed DeFET circuit used for SPECTRE simulation. The channel length and the width of the Pmos and Nmos used are $0.4\mu\text{m} / 10\mu\text{m}$ and $0.4\mu\text{m} / 1\mu\text{m}$, respectively. Fig. 3 shows the simulation results of the output voltage V_{Out} against the input voltage difference $V_{in1} - V_{in2} (\Delta V)$, where V_{in1} varies from -2.5V to 2.5V and V_{in2} is 0V .

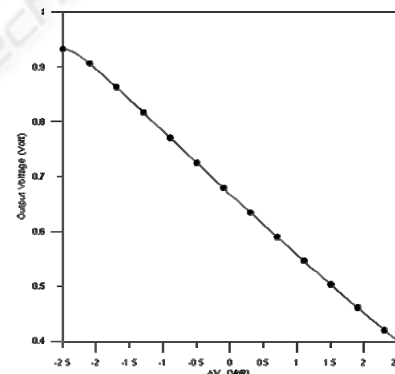


Figure 3: DC response of the DeFET.

From Fig. 3, a linear relationship between V_{Out} and ΔV can be observed. As the external electric field $E = -\Delta V / Y$, and $Y = 0.5\mu\text{m}$, Fig.4 shows the output voltage V_{Out} against the intensity of the applied electric field. We can observe that V_{Out} is linearly related to E , as we expected from the theory of the DeFET (see Eq. 1). The sensitivity can be determined from this figure as $S = \Delta V_{out} / \Delta E = 51.7(\text{mV}/\text{V}/\mu\text{m})$. If we vary V_{in1} from -2.5 to 2.5 Volt and V_{in2} from -3 to 3V olt, we can get the same

linear relationship between V_{out} and V_{in1} for different V_{in2} , as shown in Fig. 5.

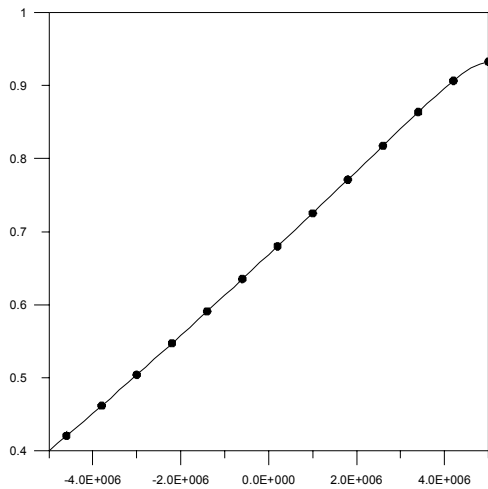


Figure 4: Output voltage versus electric field intensity.

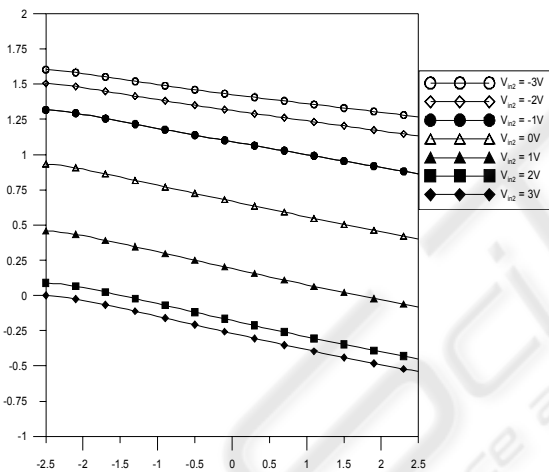


Figure 5: Spectre's simulation results.

3.2 SPICE's DC Equivalent Circuit

Fig. 6 shows the SPICE equivalent circuit of the DeFET. As it is outlined before in The DeFET's theory of operation (section 2), there are two cases of electric field. The first one is a uniform electric field case, and the second is a nonuniform electric field, both of these field cases can control the output voltage (V_{out}). The output voltage caused by the uniform case (V_{uni}) is represented by the four MOSFETs (M_1 - M_4) with the two gates are connected, see Fig. 6. In other words, V_{uni} represents the output voltage when the two gates are connected. The output current caused by a nonuniform electric field (I_{Non}), is represented by an electric field controlled current source (ECCS). I_{Non} is related to

the electric field E , and the sensitivity S by the equation ($I_{Non} = SE$).

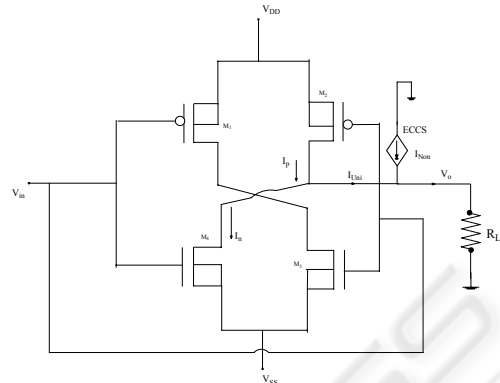


Figure 6: DeFET's SPICE equivalent circuit.

Fig. 7 shows the SPICE equivalent circuit of ECCS. In this SPICE circuit, the external electric field applied is represented as a voltage source V_{Ele} . The value of R_{Sen} is proportional to the inverse value of the sensitivity "S". I_{Non} is a current source controlled by I_1 , which caused by the nonuniform external electric field.

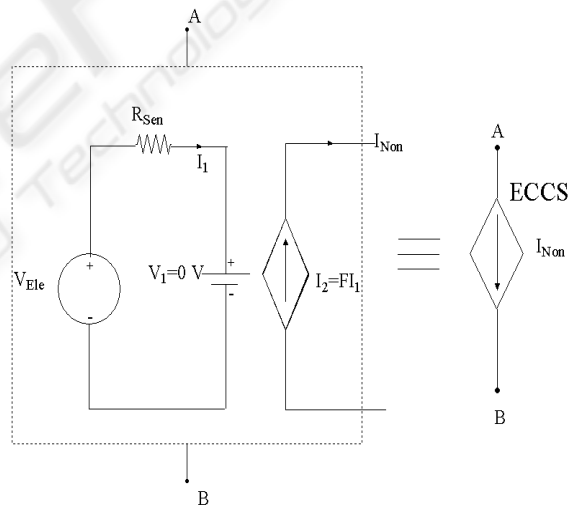


Figure 7: Electric field controlled current source (ECCS) model.

As a simple model, Fig. 8 shows this simple DC model, where the output current (I_{out}) is the summation of two dependent sources of current. The first is an electric field controlled current source (I_{Non}), which represents the nonuniform electric field, and the second is a voltage controlled current source (I_{Uni}), which represents the output current obtained when having a uniform electric field.

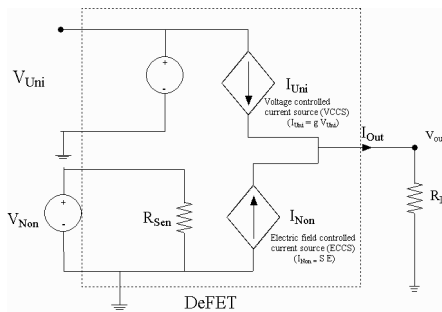


Figure 8: A simple DC model.

3.3 AC Model

Fig. 9 Shows the AC model of the DeFET, where the media is represented by a capacitor in parallel with a resistor (C_{ext}/R_{ext}). The media here can be the dielectric fluid above the DeFET sensor, or any neutral body, such as: biocells, DNA molecules, or virus, or it can be both.

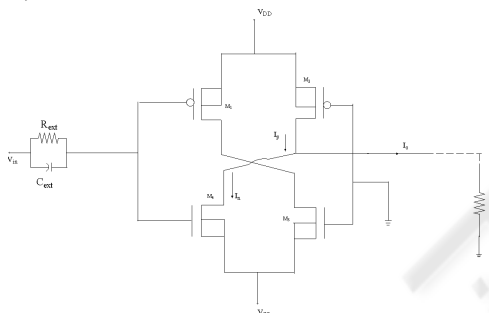


Figure 9: The AC model of the DeFET.

The AC response for different C_{ext} values is shown in Fig. 10. From this figure we can observe that the DeFET is working as a bandpass filter. The magnitude, bandwidth and the frequency range of operation of this filter depend on the external media; see Fig. 9, these factors are very important to extract useful information about the media itself. A summary of these results is shown in Table 1.

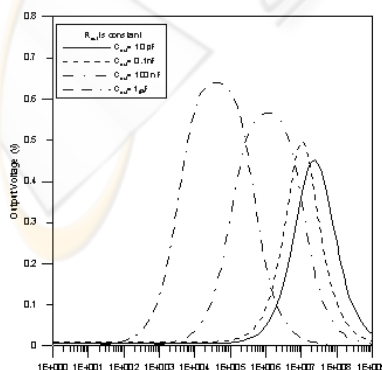


Figure 10: AC response with $R_{ext} = 500K$ Ohm and C_{ext} varies (Ghallab et al., 2006).

Table 1: Summary of the AC response when $R_{ext} = 500 K\Omega$ and C_{ext} varies.

C_{ext}	Central frequency	Bandwidth
10 pF	26.7 MHz	116 MHz
0.1 nF	10 MHz	26.59 MHz
100 nF	2.6 MHz	9.84 MHz
1 μ F	50.1 KH	311 KH

4 SIMULATION AND EXPERIMENTAL RESULTS

Fig. 11 shows the schematic input file for the PSPICE, we have used level 7 models for the used Pmos and Nmos transistors. Fig. 12 shows the simulation results of the output voltage V_{Out} against the input voltage V_3 , where V_3 varies from $-2.5V$ to $2.5V$ and V_4 varies from -3 to $3V$. From Fig. 12, V_3 represents the uniform electric field source, while V_4 represents the nonuniform electric field source. Also we can observe the linear relationship between V_{Out} and V_{in1} for different V_{in2} . In Fig. 12, both the simulation results obtained from the two different models that were proposed, i.e. using PSPICE and SPECTRE simulators, and we can observe the good agreements between these two models. Thus, both of these models can properly represent the DC response of the DeFET.

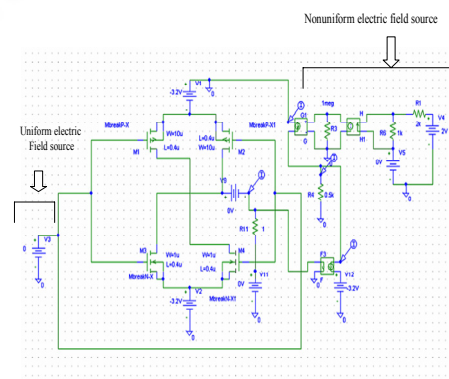


Figure 11: DeFET's PSPICE equivalent circuit.

As the external electric field $E = -\Delta V/Y$, and $Y=0.5\mu m$, Fig. 13 shows the output voltage V_{Out} against the electric field applied. We can observe that V_{Out} is linearly related to E , as we expected from the theory of the DeFET (see equation 1).

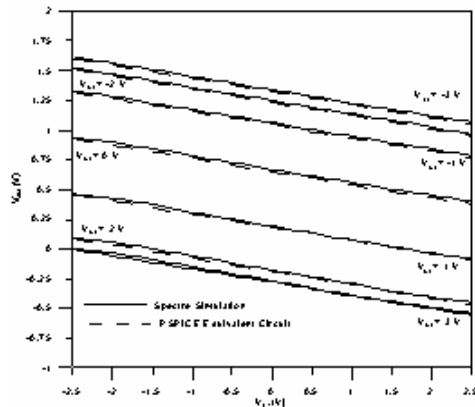


Figure 12: SPECTRE and PSPICE simulation.

As the external electric field $E = -\Delta V/Y$, and $Y=0.5\mu\text{m}$, Fig. 13 shows the output voltage V_{Out} against the electric field applied. We can observe that V_{Out} is linearly related to E , as we expected from the theory of the DeFET (see equation 1).

The proposed DeFET is implemented in the standard CMOS $0.18\text{-}\mu\text{m}$ technology. Fig. 14 shows a microscopic picture of two DeFETs and the electrodes used to apply the required electric-field pattern. To test experimentally the DC response of the DeFET, a DC voltage with different values, signs and different configuration have been applied to the four electrodes surrounding the DeFET sensors, hence, varying the magnitude and sign of the applied electric field (E) (Ghallab et al., 2006). At the output, the output voltage associated with each value of the measured electric field above the gates will be measured and compared with the simulation results, i.e., Specter’s circuit Simulator.

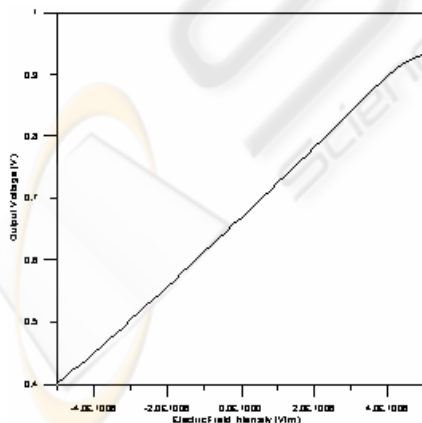


Figure 13: PSPICE Output voltage versus electric field intensity.

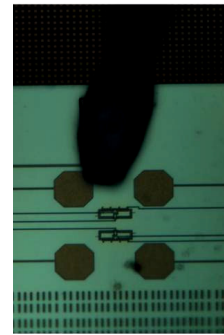


Figure 14: The die picture shows the DeFET sensor (Ghallab et al., 2006).

The result is shown in Fig.15, from which a good agreement between the experimental and the simulation results can be observed. Also, we can observe that the sensitivity of the DeFET, which is the slope of the line shown in Fig. 15, is about $51.7\text{mV}/(\text{V}/\mu\text{m})$.

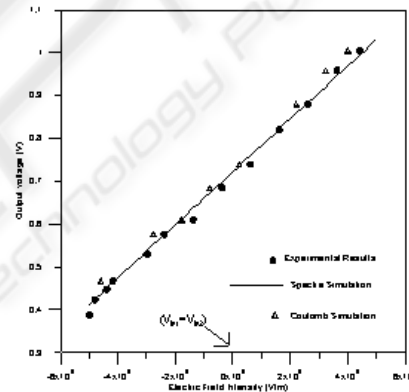


Figure 15: The DC response of the DeFET (Ghallab, 2005).

5 DeFET’S APPLICATIONS

Differential Electric Field Effect Transistor (DeFET) sensor can be used in many applications: for example, it can be used in microfluidic applications, to extract some useful properties of the fluid that is used. Also; it can be used in nonuniform electric field (Dielectrophoresis) applications to get information about the biocells that are used. To achieve this (Burt et al, 1989), DeFET can measure the disturbance that occurs from the existence of the biocells in the applied electric field; it is well known that each kind of biocell will provide a different disturbance based on its electrical properties, i.e. its conductivity and permittivity. Moreover, if we use the DeFETs in array form, i.e., array of sensors, then

we can sense the electric field at different locations. In its array form, the proposed DeFET sensor can be applied to the DNA analysis, because we can use it to detect the radius of the DNA molecule (Washizu M. et al, 1990).

6 CONCLUSIONS

This paper presents the characteristics and the alternative models of the DeFET, as a new electric field sensor. Although DeFET is not a standard device in the SPICE library, the macro models for the DeFET device is presented to evaluate the performance of circuits composed of the MOSFET and DeFET devices. The experimental results have been compared with the simulation results of the proposed models. The correctness and flexibility of the proposed SPICE models have been verified. The proposed methods are expected to make the prediction of the circuits using the DeFET and MOSFET devices possible. The proposed DeFET sensor can be used in many applications in the biomedical field.

REFERENCES

- Ghallab, Y. H. and Badaw, W. 2006, 'DeFET, A Novel Electric field Sensor for Lab-on-a-Chip and Biomedical Applications', IEEE Journal of Sensor, vol.6, no.4, pp. 1027-1037.
- Ghallab, Y. H. and Badawy, W. 2006, 'A Single CMOS Chip for Biocell Tracking, Levitation, Detection, and Characterization', International symposium on Circuit and system (ISCAS 06), pp. 3349-3352.
- Ghallab, Y. H. and Badawy, W. 2005, 'A CMOS Lab-on-a-Chip for Biomedical Applications', International symposium on Circuit and systems (ISCAS 05), pp. 1346-1349.
- Ghallab, Y. H. 2005, 'A Novel CMOS Electric Field Imager for Lab-on-a-chip and Biomedical Applications', PhD Thesis, University of Calgary, Canada.
- Burt J. P. H., Al-Ameen T. A. K., Pethig R., and Wang X., 1989, "An optical dielectrophoresis spectrometer for low frequency measurements on colloidal suspensions," *J. Phys. E, Sci. Instrum.*, vol. 22, no. 11, pp. 952-957.
- Washizu M. and Kurosawa O. 1990, "Electrostatic manipulation of DNA in microfabricated structures," *IEEE Trans. Ind. Appl.*, vol. 26, no. 6, pp. 1165-1172.